



Pope Richard J. (Orcid ID: 0000-0002-3587-837X)

Arnold Stephen R. (Orcid ID: 0000-0002-4881-5685)

Chipperfield Martyn P. (Orcid ID: 0000-0002-6803-4149)

Reddington Carly Lauren Serena (Orcid ID: 0000-0002-5990-4966)

Feng Wuhu (Orcid ID: 0000-0002-9907-9120)

Artaxo Paulo (Orcid ID: 0000-0001-7754-3036)

Sadiq Mehliyar (Orcid ID: 0000-0001-5299-3049)

Tai Amos P. K. (Orcid ID: 0000-0001-5189-6263)

**Substantial increases in Eastern Amazon and Cerrado biomass
burning-sourced tropospheric ozone**

Richard J. Pope^{1,2}, Stephen R. Arnold¹, Martyn P. Chipperfield^{1,2}, Carly L. S. Reddington¹, Edward W. Butt¹, Tim D. Keslake^{1,2}, Wuhu Feng^{1,3}, Barry G. Latter⁴, Brian J. Kerridge⁴, Richard Siddans⁴, Luciana Rizzo⁵, Paulo Artaxo⁶, Mehliyar Sadiq⁷ and Amos P. K. Tai^{7,8}

1: School of Earth and Environment, University of Leeds, Leeds, United Kingdom

2: National Centre for Earth Observation, University of Leeds, Leeds, United Kingdom

3: National Centre for Atmospheric Sciences, University of Leeds, Leeds, United Kingdom

4: Remote Sensing Group, STFC Rutherford Appleton Laboratory, Chilton, United Kingdom

5: Department of Environmental Sciences, Universidade Federal de Sao Paulo, Diadema, Brazil

6: Department of Applied Physics, Institute of Physics, University of Sao Paulo, Sao Paulo, Brazil

This article has been accepted for publication and undergone full peer review but has not been through the copyediting, typesetting, pagination and proofreading process which may lead to differences between this version and the Version of Record. Please cite this article as doi: 10.1029/2019GL084143

7: Earth System Science Programme, Faculty of Science, and Institute of Environment, Energy and Sustainability, The Chinese University of Hong Kong, Hong Kong, China

8: State Key Laboratory of Agrobiotechnology, The Chinese University of Hong Kong, Hong Kong, China

Submitted to *Geophysical Research Letters*

Abstract:

The decline in Amazonian deforestation rates and biomass burning (BB) activity (2001-2012) has been shown to reduce air pollutant emissions (e.g. aerosols) and improve regional air quality (AQ). However, in the Cerrado region (savannah grass-lands in north-eastern Brazil) satellite observations reveal increases in fire activity and tropospheric column nitrogen dioxide (an ozone precursor) during the burning season (August-October, 2005-2016), which have partially offset these AQ benefits. Simulations from a 3-D global chemistry transport model (CTM) capture this increase in NO_2 with a surface increase of ~ 1 ppbv/decade. As there are limited long-term observational tropospheric ozone records, we utilise the well-evaluated CTM to investigate changes in ozone. Here, the CTM suggests that Cerrado region surface ozone is increasing by ~ 10 ppbv/decade. If left unmitigated, these positive fire-sourced ozone trends will substantially increase the regional health risks and impacts from expected future enhancements in South American BB activity under climate change.

1. Introduction

Fire is a widely used method for land clearance in the tropics, allowing rapid conversion of regions of natural vegetation to agricultural land (Cochrane, 2003). In the Amazon, these deforestation practices led to a 15-20% decrease in forest cover between 1976 and 2010 (Hansen et al., 2013; Aragão et al., 2014; Davidson et al., 2012). Vegetation fires are a large source of reactive trace gases and aerosol to the Amazon atmosphere (Hodgson et al., 2018, Sena and Artaxo, 2015; Bela et al., 2015; Ward et al., 1992), especially during the dry season, with substantial impacts on the

atmospheric radiation balance (Sena and Artaxo, 2015; Scott et al., 2018; Thornhill et al., 2018; Kolusu et al., 2015) and surface air quality (Johnston et al., 2012; Jacobson et al., 2014; Reddington et al., 2015; Pacifico et al., 2013; Artaxo et al., 2013).

Over the period 2001 to 2012, deforestation rates in Brazil decreased by ~40% (Hansen et al., 2013) leading to improvements in particulate air quality (Reddington et al., 2015). These decreasing deforestation rates correlated with reductions in satellite-observed aerosol optical depth (AOD) over the Amazon, which were attributed to significant reductions in surface emissions of aerosol from deforestation fires (Reddington et al., 2015). Reductions in surface PM_{2.5} (mass of particulate matter with diameter less than 2.5 μm) concentrations, resulting from the reduction in fire emissions, were estimated to prevent 400-1700 premature deaths annually in South America. The reduction in fire activity is particularly evident in the arc of deforestation, around the southern edge of the Amazon Basin, where the majority of Amazon deforestation fires occur (van der Werf et al., 2017). Satellite-observed fire-burned area (FBA) in this region has decreased by 0.25-0.5 %/year between 1998 and 2015 (Andela et al., 2017). Despite these reductions in the arc of deforestation, FBA in north-eastern Brazil, has increased by 0.5-1.0% per year, resulting in increased regional pollutant emissions (Andela et al., 2017; Chen et al., 2013). This region represents the transition biome between the eastern Amazon, the Cerrado grasslands and the Caatinga desert vegetation (Santo et al., 2017). However, this region is predominantly covered by savannah grasslands and hereafter we refer to it as the “Cerrado Region” (i.e. the Cerrado biome in Figure 1a & b and the boarding regions of the Caatinga and Amazonia biomes).

As a major source of ozone precursors (nitrogen oxides (NO_x) and volatile organic compounds (VOCs)), vegetation fires have been observed to lead to enhancement in tropospheric ozone concentrations (Bela et al., 2017; Artaxo et al., 2013; Jaffe and Wigder, 2012; Kirchhoff and Marinho, 1994; Kirchhoff et al., 1996). Tropospheric ozone is an important air pollutant, which causes adverse

effects on human health (Jerrett et al., 2012; Doherty et al., 2017), crops (Hollaway et al., 2012; Van Dingenen et al., 2009) and natural vegetation (Sitch et al., 2007). Deforestation fires tend to be large in scale (due to extensive above-ground biomass) with a greater amount of smouldering, while savannah fires tend to be smaller and burn at higher temperatures with more flaming combustion (Hodgson et al., 2018; Alencar et al., 2015; Longo et al., 2009). Consequently, these different fire characteristics can result in very different emissions. For instance, emission factors (i.e. mass of trace gas/aerosol emitted per mass of dry matter burnt) for deforestation fires, release larger quantities of primary aerosol emissions (13.0 gkg^{-1}) than savannah fires (8.5 gkg^{-1}), while the converse is the case for NO_x emissions (deforestation emission factor = 2.55 gkg^{-1} and savannah emission factor = 3.9 gkg^{-1}) (Akagi et al., 2011). Therefore, understanding how changes in fire activity impact NO_x and ozone pollution requires knowledge of the underlying vegetation type and emission characteristics.

It is only recently, in the satellite era, that space-borne observations from various missions have made it possible to study long-term changes in global tropospheric composition. Here, we present the first study using these long-term (2005-2016) records, in conjunction with a chemistry transport model (CTM), to investigate the impact of changing wildfire/biomass burning (BB) activity on tropospheric ozone air quality across the Amazon during the BB season (August-September-October, ASO). We exploit satellite measurements of tropospheric nitrogen dioxide (NO_2) and fire activity, as well as new state-of-the-art lower tropospheric ozone retrievals. Our focus is on detecting and analysing trends in tropospheric/surface ozone and its precursors to investigate the impact on regional AQ. Section 2 introduces the satellite measurements and CTM used in this study, section 3 presents our results and the conclusions are discussed in section 4.

2. Methods and Data:

2.1. Satellite Data

We use satellite measurements of tropospheric column NO₂ (TCNO₂) and sub-column (0-6 km) ozone (SCO₃) from the Ozone Monitoring Instrument (OMI) from 2005-2016. OMI is a nadir viewing instrument on-board NASA's Aura satellite (2004-present) (Boersma et al., 2007). The OMI TCNO₂ data was downloaded as Level 2 swath data from the Tropospheric Emissions Monitoring Internet Service (TEMIS, www.temis.nl). The SCO₃ data was provided by the Rutherford Appleton laboratory (RAL), which uses an optimal estimation technique (Miles et al., 2015) to produce a state-of-the-art product with peak vertical sensitivity in the lower troposphere. Aura is polar orbiting with an approximate local overpass time of 13.30 and OMI has nadir-viewing spectral ranges of 270-500 nm (Boersma et al., 2011). All data sets have been quality controlled for geometric cloud fraction less than 0.2, good quality flags and the OMI row anomalies (Braak, 2010) where applicable. Detailed analysis of TCNO₂ retrieval uncertainties is provided by Boersma et al., (2004), while Bousserez (2014) quantify the impact of biomass burning aerosol uncertainty on retrieved TCNO₂. Miles et al., (2015) provide error/uncertainty analysis on the retrieval scheme used for the RAL OMI SCO₃ product. These satellite data sets were mapped onto high-resolution spatial grids of 0.05° × 0.05° for TCNO₂ and 1.0° × 1.0° for SCO₃ (Pope et al., 2018). Global Ozone Monitoring Experiment – 2 (GOME-2) TCNO₂ data was also acquired from TEMIS as a Level 3 monthly mean gridded product for August-September-October (ASO) 2007-2016, to confirm that the Cerrado Region TCNO₂ positive trends (**Figure 2a**) were realistic and not an artefact of the OMI row anomaly.

We use two different satellite-derived fire activity datasets to investigate regional patterns in fires and their trends over time. These are fire-burned-area (FBA) from the Global Fire Emissions Database (GFED vn4.0 (van der Werf et al., 2017) and fire radiative power (FRP) from the Global Fire Assimilation System (GFAS vn1.2; Kaiser et al., 2012). Both fire products are derived from Moderate Resolution Imaging Spectroradiometer (MODIS) measurements, on-board NASA's Aqua and Terra satellites (Remer et al., 2005) and are used to produce gas-phase and aerosol emissions from fires through application of emissions factors (Wooster et al., 2018). While GFAS only provides FRP and

total emissions, GFED provides information on different vegetation types burned, including contributions from deforestation and savannah fires.

2.2. TOMCAT Model Setup and Evaluation

The TOMCAT global off-line chemical transport model (CTM) (Chipperfield, 2006) is forced by ECMWF ERA-Interim reanalysis meteorology (Dee et al., 2011) and has a horizontal spatial resolution of $2.8^{\circ} \times 2.8^{\circ}$ with 31 vertical levels up to 10 hPa. The model includes detailed tropospheric chemistry, including 229 gas-phase reactions and 82 advected tracers (Monks et al., 2017), and heterogeneous chemistry driven by size-resolved aerosol from the GLOMAP module (Mann et al., 2010). Simulations used here include anthropogenic emissions from the Coupled Model Intercomparison Project Phase 6 (CMIP6) (Hosely et al., 2018) and fire emissions from GFED vn4.0 (van der Werf et al., 2017). Biogenic Volatile Organic Compounds (VOCs) emissions are from the Chemistry-Climate Model Initiative (CCMI) (Morgenstern et al., 2017).

TOMCAT surface/tropospheric ozone was evaluated against surface observations from Manaus (60.2°W , 2.6°S) in the Amazon (2010-2011). During the BB season (ASO), the model successfully captures peak observed surface ozone concentrations of 13-15 ppbv. However, between January and May there is systematic positive bias of ~ 5 ppbv (although this is within the observational variability). Comparisons with aircraft observations from the the South AMerican Biomass Burning Analysis (SAMBBA) campaign (Darbyshire et al., 2019) (September-October, 2012) show the model successfully reproduces the boundary layer vertical ozone profile between 30-45 ppbv, with a slight positive bias of 2-3 ppbv. These observations and comparison are also consistent with ozonesondes from Natal (2007-2008). More details on the model evaluation are located in the **SM 2**.

Overall, the TOMCAT model successfully captures the Amazon ozone seasonality and absolute concentrations in the lower troposphere, giving some confidence in the ozone simulations used to investigate long-term changes in surface ozone in the following analysis.

3. Results

3.1. Satellite fire emission signals and trend detection

The period of peak fire activity over the Amazon occurs during ASO (Hodgson et al., 2018; van der Werf et al., 2017; Kaiser et al., 2012), when FBA (**Figure 1a**) and FRP (**Figure 1c**) reach over 10% and 100 mW/m², respectively. In contrast, during the non-BB season (February-March-April, FMA), there are minimal fire signals, peaking at <1% (**Figure 1b**) and 10 mW/m² (**Figure 1d**). Substantial fire-related TCNO₂ signals (2.5-4.0 × 10¹⁵ molecules/cm², **Figure 1e**) are present across the Amazon during ASO, while in FMA TCNO₂ concentrations are less than 1.0 × 10¹⁵ molecules/cm² (**Figure 1f**). During ASO peak TCNO₂ is located over the Cerrado region where savannah-type fires (both natural and anthropogenic) burn at high temperatures (Hodgson et al., 2018) releasing large quantities of NO_x (Akagi et al., 2011). There will also be contributions from deforestation and agricultural fires (e.g. de Araújo et al., 2019). In comparison, TCNO₂ hotspots over large cities (e.g. São Paulo and Rio De Janeiro) show limited seasonality, remaining above 5.0 × 10¹⁵ molecules/cm² year-round. The SCO₃ ASO signal is more homogeneous, consistent with ozone being a secondary NO_x-induced pollutant formed downwind of source regions. A clear SCO₃ enhancement (22-25 Dobson units, DU) is present during ASO over the Amazon compared with FMA (12-18 DU). SCO₃ over the South Atlantic is also elevated (over 22 DU) in ASO as a result of ozone-enriched outflow from the southern African biomass burning (Moxim and Levy, 2000).

A long-term trend analysis (**Figure 2**) shows significant increases in both fire activity and TCNO₂ across the Cerrado Region. Trends are calculated using a linear least-squares fit over the ASO composition average for each year between 2005 and 2016, where we remove extreme

drought/anomalous fire years (e.g. 2005, 2007, 2010 and 2012; hereafter defined as ED-AF). Though the 2015 intense positive El Niño-Southern Oscillation (ENSO) event substantially enhanced drought conditions in the Central Amazon (Anderson et al., 2018), it had a limited impact on fire activity over our primary region of interest (black box in Figure 1a – see **SM 1**). Hence, 2015 was not defined as ED-AF (see **SM 1**). We follow the approach of Reddington et al., (2015) and remove ED-AF years from our analysis as they represent different emission regimes when compared to the normal state (Aragão et al., 2014). For aerosol emissions, Reddington et al., (2015) found that ED-AF years were 1.5-2.8 times greater than normal years, while for NO_x emissions we find a factor increase of 14-15. This avoids skewing of the long-term trends due to larger than usual fire activity and tropospheric pollutant loading in those years. Black polygon-outlined regions in **Figure 2** show significant trends at and above the 90% confidence level ($>90\%CL$, $trend/\sigma_{trend} > 1.645$). Artificial background TCNO₂ trends (i.e. OMI row anomaly; Braak, 2010) have been removed from the OMI time series (**SM 1**). Where significant TCNO₂ trends exist, there are insignificant trends in the stratospheric slant NO₂ column and in the tropospheric air mass factor.

Significant positive trends in FBA (**Figure 2a**), FRP (**Figure 2b**) and TCNO₂ (**Figure 2c**) range between 0.3-0.7 %/year, 2-5 mW/m²/year and 0.1-0.15 ×10¹⁵ molecules/cm²/year, respectively, potentially driven by changes in Cerrado savannah-type fire activity. Given that all three data sets have spatially consistent trends, it provides us with confidence that the detected TCNO₂ trends are related to fire activity. In the arc of deforestation region, significant (>90% CL) negative trends are also found in all three datasets, consistent with previous studies (Reddington et al., 2012), which identified decreases in deforestation fires and satellite-observed AOD between 2001 and 2012. Though the positive FBA and TCNO₂ signals are spatially less extensive than those of the FRP and AOD negative trends.

As the significant fire activity and TCNO₂ positive trends over the Cerrado Region are spatially sporadic and disjointed, regional trends (**Figure 2d**) in FBA and TCNO₂ were determined from the

black-outlined region in **Figure 2a**. The variability (standard deviation) in the regional FBA and TCNO₂ typically ranges between 150-190% and 40-60% of the mean values, respectively, in non ED-AF years. Here, there are significant regional trends (99% CL) in both FBA and TCNO₂. The TCNO₂ regional trend from the Global Ozone Monitoring Experiment – 2 (GOME-2) satellite instrument also increases significantly over time (2007-2016), supporting the OMI TCNO₂ results. By sub-sampling OMI TCNO₂ under pixels with FBA >1.0%, concentrations are larger by approximately 0.5×10^{15} molecules/cm², highlighting a similar significant positive trend (red dashed line). This strongly suggests that increasing regional TCNO₂ concentrations are being driven by increased fire activity as TCNO₂ is larger in fire-classified pixels with a consistent significant positive trend.

Analysis of trends in GFED NO_x emissions, which are based on FBA, for ASO indicates that increases in GFED-defined savannah-type fires are likely responsible for the increases in TCNO₂ over the Cerrado Region. **Figure 3a** shows the GFED NO_x emissions trends for all fire types for 2005-2016 with ED-AF years removed, and shows significant positive trends (0.05-0.15 g/m²/year) over the Cerrado Region, consistent with the FBA, FRP and TCNO₂. When split into fire types, agricultural fires (**Figure 3d**) show negligible trends, while deforestation fires (**Figure 3c**) give spatially incoherent trends across the Amazon (partial spatial agreement with savannah fires over portions of the Cerrado Region e.g. around 50°W, 12°S suggesting a range of different vegetation fire-types driving the positive trends seen in **Figure 2** and **3**). However, the significant positive NO_x emission trends (0.05-0.1 g/m²/year) from savannah fires (**Figure 3b**) are closely related to the magnitude and spatial pattern of the trends in **Figure 3a**. Though it should be noted that the GFED fire-type classifications can be subject to uncertainties (van der Werf et al., 2017). Missed or false fire detections in will also introduce further emission uncertainties (e.g. particulate emissions; Reddington et al., (2016)).

3.2. Model simulated NO₂ and ozone

TOMCAT model simulations (2005-2016, **Figure 4**), using annual varying GFED vn4.0 fire emissions, are used to investigate the impact of increased fire activity (predominantly savannah-type fires) on air quality over the Cerrado region, and the wider surrounding Amazon area, given the limited observational spatial and temporal coverage. Neither the surface or aircraft data provide long-term records and the ozonesondes are from Natal (a coastal city). The OMI SCO_3 observations provide valuable seasonal information over the wider Amazon, but are not sensitive enough to detect finer scale changes (e.g. for the Cerrado region) in ozone with time. However, evaluation of TOMCAT tropospheric ozone using these observations (surface sites, aircraft data and ozonesondes; **see SM 2**) show that the model is able to capture the surface ozone seasonal cycle and reproduce the lower tropospheric vertical profile.

Over the 2005-2016 period, fire-sourced ozone contributes approximately an extra 10-15 ppbv to Amazon surface ozone concentrations during the BB season. **Figure 4a** shows the difference between the TOMCAT “fire-on” and “fire-off” simulations, where fires have substantially contributed to the surface ozone budget in ASO, consistent with the ozone seasonality in the observations. During ASO, the 2005-2016 average surface concentrations range between 40-50 ppbv in the “fire-on” simulation, while decreasing to under 20 ppbv when fire sources are switched off (“fire-off”, **see SM 3**). The red and blue dashed regions in **Figure 4d** represent the Eastern Amazon and Wider Amazon, respectively, and highlight regions where we have detected long-term fire-sourced ozone enhancements. During ASO, the domain average fire-source ozone contribution ranges between 10-15 ppbv and 5-11 ppbv for the Eastern Amazon and Wider Amazon regions (**Figure 4b**). This implies that approximately 50-60% of the ASO surface ozone is from fire sources (**see SM 3**). The ASO Eastern Amazon ozone contributions tends to be larger as more NO_x is emitted from the predominantly savannah-type fire regimes (i.e. **Figure 3b**), when compared with the Wider Amazon region.

Trends in model surface ASO mean NO₂ show significant (>90%CL) increases (>0.1 ppbv/year) over the Cerrado region and decreases (-0.03 to -0.01 ppbv/year) in the arc of deforestation (**Figure 4a**).

As expected, the short NO₂ lifetime means that these trends are highly correlated with those in GFED v4.0 NO_x fire emissions (**Figure 3a**). The significant increase in Cerrado fire-related NO_x, in the presence of VOC concentrations (both biogenic emissions from vegetation and emissions from fires), yields significant increases in simulated ozone (over 1.0 ppbv/year, **Figure 4b**). However, insignificant decreases (-0.2 to 0.0 ppbv/year) and increases (0.1-0.3 ppbv/year) occur over the arc of deforestation and western Amazon, respectively. Model-simulated eastern Brazil surface NO₂ and ozone (same region in **Figure 2a, SM 3**) also show significant regional positive trends (>90% CL).

4. Discussion and Conclusions

Overall, our results show that there has been a significant increase in fire activity in the Cerrado region (savannah grasslands) of North-eastern Brazil, between 2005 and 2016, yielding substantial increases in fire-related tropospheric pollutants (i.e. NO₂ and ozone). This is important as it highlights different behaviour compared with the “arc of deforestation” region (the south-western Amazon reaching to the north-eastern flank), where a decline in deforestation fires has yielded lower particulate matter emissions and reduced the corresponding health risks (Reddington et al., 2015). As there are limited observations of surface/tropospheric ozone in the Amazon, well-evaluated model simulations offer a method to quantify long-term changes in surface ozone concentrations. In the Cerrado region, TOMCAT simulations suggest considerable long-term increases in fire-sourced surface ozone (~1.0 ppbv/year equating to ~10-12 ppbv regionally over the study period), predominantly from increased burning of savannah grasslands in the Cerrado Region, but also with contributions from deforestation fires.

Should these fire activities continue to intensify, as is currently seen in Brazil (TerraBrasilis, 2019; NASA, 2019), the health risks and socioeconomic impacts associated with fire-sourced ozone pollution may increase substantially. This will be confounded by the high probability of more

frequent and intense drought BB from future climate change (Page et al., 2017) and land-use change (Fonseca et al., 2019), as well as expected increases in the South American population (United Nations, 2017). The enhanced ozone will also likely further damage vegetation and reduce photosynthesis (Sitch et al., 2007; Pacifico et al., 2015) leading to reductions in crop yields (Hollaway et al., 2012). These effects combined could have substantial impacts on natural vegetation, agriculture, and public health, with potential degradation in ecosystem services and economic losses. Therefore, targeted policies on controlling Cerrado biomass burning would be beneficial to generate local and regional air quality improvements with associated public and ecological health benefits.

Acknowledgements:

This work was supported by the UK Natural Environment Research Council (NERC) by providing funding for the National Centre for Earth Observation (NCEO). We also acknowledge funding from the NERC PROMOTE project (grant number: NE/P016421/1). TOMCAT modelling development was supported by the National Centre for Atmospheric Science (NCAS). Simulations were performed on the national Archer and Leeds ARC HPC systems. Collaboration between Leeds and CUHK was supported by the Research Development Fund (Project ID: 6904209) of the Worldwide Universities Network. We acknowledge the use of the Tropospheric Emissions Monitoring Internet Service (TEMIS: <http://www.temis.nl/airpollution/no2.html>) OMI TCNO₂ (DOMINO v2.0) data and the Rutherford Appleton Laboratory (RAL) OMI SCO₃ data. We also acknowledge the use of fire activity data from the Global Fire Emissions Database (GFED), which were obtained from <https://www.globalfiredata.org/index.html>. FRP data comes from the ECMWF CAMS Global Fire Assimilation System, which can be found at <http://apps.ecmwf.int/datasets/data/cams-gfas/>. Airborne data from The South American Biomass Burning Analysis (SAMBBA) campaign (<https://www.ncas.ac.uk/en/campaigns/651-sambba>) was obtained using the BAe-146-301 Atmospheric Research Aircraft (ARA) flown by Directflight Ltd and managed by the Facility for

Airborne Atmospheric Measurements (FAAM), which is a joint entity of NERC and the Met Office (accessed from <https://catalogue.ceda.ac.uk/uuid/2ff89840a89840868acff801f8859451>). We also acknowledge funding from FAPESP – Fundação de Amparo à Pesquisa do Estado de São Paulo, grants number 2017/17047-0,2012/14437-9. Ozonesonde data from Natal was part of the SHADOZ project (<https://tropo.gsfc.nasa.gov/shadoz/>). Model emissions inventories were provided by Louisa K. Emmons from the National Center for Atmospheric Research, USA. TOMCAT simulations are publically available at: http://homepages.see.leeds.ac.uk/~earrjpo/open_access_files/ as netcdf files.

References:

Akagi, S. K., Yokelson, R. J., Wiedinmyer, C., Alvarado, M. J., Reid, J. S., Karl, T., et al. (2011). Emission factors for open and domestic biomass burning for use in atmospheric models. *Atmospheric Chemistry and Physics* **11**, 4039-4072. <https://doi.org/10.5194/acp-11-4039-2011>.

Alencar, A. A., Brando, P. M., Asner, G. P. & Putz, F. E. (2015). Landscape fragmentation, severe drought, and the new Amazon forest fire regime. *Ecological Applications* **25**(6), 1493-1505. <https://doi.org/10.1890/14-1528.1>.

Andela, N., Morton, D. C., Giglio, L., Chen, Y., van der Werf, G. R., Kasibhatla, P. S., et al. (2017). A human-driven decline in global burned area. *Science* **356**, 1356-1362. DOI: 10.1126/science.aal4108.

Aragão, L. E. O. C., Poulter, B., Barlow, J. B., Anderson, L. O., Malhi, Y., Saatchi, S., et al. (2014). Environmental change and the carbon balance of Amazonian forests. *Biological Reviews* **89**, 913-931. <https://doi.org/10.1111/brv.12088>.

Artaxo, P., Rizzo, L. V., Brito, J. F., Barbosa, H. M. J., Arana, A., Sena, E. T., et al. (2013). Atmospheric aerosols in Amazonia and land use change: from natural biogenic to biomass burning conditions.

Faraday Discussions **165**, 203-235. DOI: 10.1039/C3FD00052D.

Bela, M. M., Longo, K. M., Freitas, S. R., Moreira, D. S., Beck, V., Wofsy, S. C., et al. (2015). Ozone production and transport over the Amazon basin during the dry-wet and wet-dry transition seasons.

Atmospheric Chemistry and Physics **15**, 757-782. <https://doi.org/10.5194/acp-15-757-2015>.

Boersma, K. F., Eskes, H. J. and Brinksma, E.J. (2004). Error analysis for tropospheric NO₂ retrievals from space, *Journal of Geophysical Research*, **109** (D04311), doi:10.1029/2003JD00362.

Boersma, K. F. et al. (2007). Near-real time retrievals of tropospheric NO₂ from OMI. *Atmospheric Chemistry and Physics* **7**, 2103-2118 (2007). <https://doi.org/10.5194/acp-7-2103-2007>.

Boersma, K. F., Eskes, H. J., Veefkind, J. P., Brinksma, E. J., van der A., R. J., Sneep, M., et al. (2011).

An improved tropospheric NO₂ column retrieval algorithm for the Ozone Monitoring Instrument.

Atmospheric Measurement Techniques **4**, 1905-1928. <https://doi.org/10.5194/acp-7-2103-2007>.

Braak, R. (2010). Row Anomaly Flagging Rules Lookup Table, *KNMI Technical Document TN-OMIE-KNMI-950*.

Bousserez, N. (2014). Space-based retrieval of NO₂ over biomass burning regions: quantifying and reducing uncertainties, *Atmospheric Measurement Techniques* **7**, 3431-3444,

<https://doi.org/10.5194/amt-7-3431-2014>.

Chen, Y., Morton, D. C., Jin, Y., Collatz, G. J., Kasibhatla, P. S., van der Werf, G. R., et al. (2013). Long-term trends and interannual variability of forest, savannah and agricultural fires in South America.

Carbon Management **4**(6), 617-638. <https://doi.org/10.4155/cmt.13.61>.

Chipperfield, M. P. (2006). New version of the TOMCAT/SLIMCAT off-line chemistry transport model Intercomparison of stratospheric trace experiments. *Quarterly Journal of the Royal Meteorological Society* **132**, 1179-1203. <https://doi.org/10.1256/qj.05.51>.

Cochrane, M. A. (2003). Fire sciences for rainforests. *Nature* **421**, 913-919.

<https://doi.org/10.1038/nature01437>.

Darbyshire, E., Morgan, W. T., Allan, J. D., Liu, D., Flynn, M. J., Dorsey, J. R., et al. (2019). The vertical distribution of biomass burning pollution over tropical South America from aircraft in situ measurements during SAMBBA. *Atmospheric Chemistry and Physics* **19**, 5771-5790.

<https://doi.org/10.5194/acp-19-5771-2019>.

Davidson, E. A., de Araujo, A. C., Artaxo, P., Balch, J. K., Brown, I. F., Bustamante, M. M. C., et al. (2012). The Amazon Basin in transition. *Nature* **481**, 321-328. <https://doi.org/10.1038/nature10717>.

de Araújo, M. L. S., Sano, E. E., Bolfe, E. L., Santos, J. R. N., dos Santos, J. S. & Silva, F. B. (2019).

Spatiotemporal dynamics of soybean crop in the Matopiba region, Brazil (1990-2015). *Land Use*

Policy **80**, 57-67, <https://doi.org/10.1016/j.landusepol.2018.09.040>.

Dee, D. P., Uppala, S. M., Simmons, A. J., Berrisford, P., Poli, P., Kobayashi, S., et al. (2011). The ERA-Interim reanalysis: configuration and performance of the data assimilation system. *Quarterly Journal of the Royal Meteorological Society* **137**, 553-597. <https://doi.org/10.1002/qj.828>.

Doherty, R. M., Heal, M. R. & O'Connor, F. M. (2017). Climate change impacts on human health over Europe through its effect on air quality. *Environmental Health* **16**(118), 33-44. <https://doi.org/10.1186/s12940-017-0325-2>.

Fonseca, M. G., Alves, L. M., Aguiar, A. P. D., Arai, E., Anderson, L. O., Rosan, T. M., Shimabukuro, Y. E. & Aragão, L. E. O. C. (2019). Effects of climate and land-use change scenarios on fire probability during the 21st century in the Brazilian Amazon. *Global Change Biology* **25** (9), 2931–294, doi: 10.1111/gcb.14709.

Global Forest Watch. (2019). Brazil Biomes. http://data.globalforestwatch.org/datasets/54ec099791644be4b273d9d8a853d452_4/data.

Hansen, M. C., Potapov, P. V., Moore, R., Hancher, M., Turubanova, S. A., Tyukavina, A., et al. (2013). High-Resolution Global Maps of 21st-Century Forest Cover Change. *Science* **342**, 850-853. DOI: 10.1126/science.1244693.

Hodgson, A. K., Morgan, W. T., O'Shea, S., Bauguitte, S., Allan, J. D., Darbyshire, E., et al. (2018). Near-field emission profiling of tropical forest and Cerrado fires in Brazil during SAMBBA 2012. *Atmospheric Chemistry and Physics* **18**, 5619-5638. <https://doi.org/10.5194/acp-18-5619-2018>.

Hollaway, M. J., Arnold, S. R., Challinor, A. J. & Emberson, L. D. (2012). Intercontinental trans-boundary contributions to ozone-induced crop yield losses in the North Hemisphere. *Biogeosciences* **9**, 271-2929. <https://doi.org/10.5194/bg-9-271-2012>.

Hosely, R. M., Smith, S. J., Feng, L., Kllmont, Z., Janssens-Maenhout, G., Pitkanen, T., et al. (2018). Historical (1750-2014) anthropogenic emissions of reactive gases and aerosols from the Community Emissions Data System (CEDS). *Geoscientific Model Development* **11**, 369-408. <https://doi.org/10.5194/gmd-11-369-2018>.

Jacobson, L. S. V., Hacon, S. S., Castro, H. A., Ignotti, E., Artaxo, P., Hilario, P., et al. (2014). Acute Effects of Particulate Matter and Black Carbon from Seasonal Fires on Peak Expiratory Flow of School Children in the Brazilian Amazon. *Public Library of Science* **9**(8), 1-14. <https://doi.org/10.1371/journal.pone.0104177>.

Jaffe, D. A. & Wigder, N. L. (2012). Ozone production from wildfires: A critical Review. *Atmospheric Environment* **51**, 1-10. <https://doi.org/10.1016/j.atmosenv.2011.11.063>.

Jerrett, M., Burnett, R. T., Pope, C. A., Ito, K., Thurston, G., Krewski, D., et al. (2009). Long-Term Ozone Exposure and Mortality. *The New England Journal of Medicine* **360**(11), 1085-1095. DOI: 10.1056/NEJMoa0803894.

Johnston, F. H., Henderson, S. B., Chen, Y., Randerson, J. T., Marlier, M., Defries, R. S., et al. (2012). Estimated Global Mortality Attributable to Smoke from Landscape Fires. *Environmental Health Perspectives* **120**, 695-701. doi: 10.1289/ehp.1104422.

Kaiser, J. W., Hell, A., Andreae, M. O., Benedetti, A., Chubarova, N., Jones, L., et al. (2012). Biomass burning emissions estimated with a global fire assimilation system based on observed fire radiative power. *Biogeosciences* **9**, 527-554. <https://doi.org/10.5194/bg-9-527-2012>.

Kirchhoff, V. W. J. H. and Marinho, E. V. A. (1994). Layer enhancements of tropospheric ozone in regions of biomass burning. *Atmospheric Environment* **28(1)**, 69-74.

doi:[https://doi.org/10.1016/1352-2310\(94\)90023-X](https://doi.org/10.1016/1352-2310(94)90023-X).

Kirchhoff, V. W. J. H., Alves, J. R., da Silva, F. R., and Fishman, J. (1996). Observations of ozone concentrations in the Brazilian cerrado during the TRACE A field expedition, *Journal of Geophysical Research*, **101(D19)**, 24029- 24042, doi:10.1029/95JD03030.

Kolusu, S. R., Marsham, J. H., Mulcahy, J., Dunning, C., Bush, M., & Spracklen, D. V. (2015). Impacts of Amazonian biomass burning aerosols assessed from short-range weather forecasts. *Atmospheric Chemistry and Physics* **15**, 12251-12266. doi:10.5194/acp-15-12251-2015.

Longo, K. M., Freitas, S. R., Andreae, M. O., Yokelson, R. & Artaxo, P. (2009). *Biomass Burning in Amazonia: Emissions, Long-Range Transport of Smoke, and its Regional and Remote Impacts* (Amazonia and Global Change, Volume 186).

Mann, G. W., Carslaw, K. S., Spracklen, D. V., Ridley, D. A., Manktelow, P. T., Chipperfield, M. P., et al. (2010). Description and evaluation of GLOMAP-mode: a modal global aerosol microphysics model for the UKCA composition-climate model. *Geoscientific Model Development* **3**, 519-551.

<https://doi.org/10.5194/gmd-3-519-2010>.

Miles, G. M., Siddans, R., Kerridge, B. J., Latter, B. G. & Richards, N. A. D. (2015). Tropospheric ozone and ozone profiles retrieved from GOME-2 and their validation. *Atmospheric Measurement Techniques* **8**, 385-398. <https://doi.org/10.5194/amt-8-385-2015>.

Monks, S. A., Arnold, S. R., Hollaway, M. J., Pope, R. J., Wilson, C., Feng, W., et al. (2017). The TOMCAT global chemistry transport model v1.6: description of chemical mechanism and model evaluation. *Geoscientific Model Development* **10**, 3025-3057. <https://doi.org/10.5194/gmd-10-3025-2017>.

Morgenstern, O., Hegglin M, I., Rozanov, E., O'Connor, F, M., Abraham, N. L., Akiyoshi, H., et al. (2017). Review of the global models used with phase 1 of the Chemistry-Climate Model Initiative (CCMI). *Geoscientific Model Development* **10**, 639-671. <https://doi.org/10.5194/gmd-10-639-2017>.

Moxim, W. J. & Levy, H. (2000). A model analysis of tropical South Atlantic Ocean tropospheric ozone maximum: The interaction of transport and chemistry. *Journal of Geophysical Research* **105**(D13), 17,393-17,415. <https://doi.org/10.1029/2000JD900175>.

NASA. (2019). Uptick in Amazon Fire Activity in 2019. <https://www.earthobservatory.nasa.gov/images/145498/uptick-in-amazon-fire-activity-in-2019>.

Pacifico, F., Folberth, G, A., Sitch, S., Haywood, J. M., Rizzo, L, V., Malavelle, F. F. & Artaxo, P. (2015). Biomass burning related ozone damage on vegetation over the Amazon forest: a model sensitivity study. *Atmospheric Chemistry and Physics* **15**, 2791-2804. <https://doi.org/10.5194/acp-15-2791-2015>.

Page, Y. L., Morton, D., Hartin, C., Bond-Lamberty, B., Pereira, J. M. C., Hurtt, G. & Asrar, G. (2017). Synergy between land use and climate change increases future fire risk in Amazon forests. *Earth System Dynamics* **8**, 1237-1246. <https://doi.org/10.5194/esd-8-1237-2017>.

Pope, R. J., Arnold, S. R., Chipperfield, M. P., Latter, B. G., Siddans, R. & Kerridge, B. J. (2018). Widespread changes in UK air quality observed from space. *Atmospheric Science Letters* **19**, e817. <https://doi.org/10.1002/asl.817>.

Reddington, C. L., Butt, E. W., Ridley, D. A., Artaxo, P., Morgan, W. T., Coe, H. & Spracklen, D. V. (2015). Air quality and human health improvements from reductions in deforestation-related fires in Brazil, *Nature Geoscience* **8**, 768-773. <https://doi.org/10.1038/ngeo2535>.

Reddington, C. L., Spracklen, D. V., Artaxo, P., Ridley, D. A., Rizzo, L. V. & Arana, A. (2016). Analysis of particulate emissions from tropical biomass burning using a global aerosol model and long-term surface observations. *Atmospheric Chemistry and Physics* **16** (17), 11083-11106, DOI:10.5194/ACP-16-11083-2016.

Remer, L. A., Kaufman, Y. J., Tanré, D., Mattoo, S., Chu, D. A., Martins, J. V., et al. (2005). The MODIS Aerosol Algorithm, Products and Validation. *Journal of the Atmospheric Sciences* **62**, 947-973. <https://doi.org/10.1175/JAS3385.1>.

Santo, M. A., Filho, J. B. S. F., Filho, J. E. R. V. & Ywata, A. X. C. (2017). Setor Agropecuário Brasileiro Pós-Novo Código Florestal: uma simulação de impactos econômicos. *Instituto de Pesquisa Econômica Aplicada* **2320**, 1-46.

Sena, E. T. & Artaxo, P (2015). A novel methodology for large-scale daily assessment of direct radiative forcing of smoke aerosols. *Atmospheric Chemistry and Physics* **15**, 5471-5483.

<https://doi.org/10.5194/acp-15-5471-2015>.

Scott, C. E., Monks, S, A., Spracklen, D. V., Arnold, S. R., Forster, P, M., Rap, A., et al. (2018). Impacts on short-lived climate forcers increases projected warming due to deforestation. *Nature*

Communications **9**, 157. <https://doi.org/10.1038/s41467-017-02412-4>.

Sitch, S., Cox, P. M., Collins, W. J. & Huntingford, C. (2007). Indirect radiative forcing of climate change through ozone effects on the land carbon sink. *Nature* **448**, 791-795.

<https://doi.org/10.1038/nature06059>.

Terrabrasilia. (2019). Analyses – Legal Amazon.

<http://terrabrasilis.dpi.inpe.br/app/dashboard/alerts/legal/amazon/aggregated/>.

Thornhill, G. D., Ryder, C. L., Highwood, E. J., Shaffrey, L. C. & Johnson, B. T. (2018). The effect of South American biomass burning aerosol emissions on regional climate. *Atmospheric Chemistry and*

Physics **18**, 5321-5342. <https://doi.org/10.5194/acp-18-5321-2018>.

United Nations (UN). (2017). World Population Prospects: The 2017 Revisions - key finds and advice tables.

van der Werf, G. R., Randerson, J. T., Giglio, L., van Leeuwen, T. T., Chen, Y., Rogers, B, M., et al.

2017. Global fire emission estimates during 1997-2016. *Earth System Science Data* **9**, 697-720.

<https://doi.org/10.5194/essd-9-697-2017>.

Van Dingenen, R., Dentener, F. J., Raes, F., Krol, M, C., Emberson, L. & Cofala, J. (2009). The global impact of ozone on agriculture crop yields under current and future air quality legislation.

Atmospheric Environment **43**(3), 604-618. <https://doi.org/10.1016/j.atmosenv.2008.10.033>.

Ward, D. E., Susott, R. A., Kauffman, J. B., Babbitt, R. E., Cummings, D. L., Dias, B., Holben, B. N., Kaufman, Y. J., Rasmussen, R. A., and Setzer, A. W. (1992). Smoke and fire characteristics for cerrado and deforestation burns in Brazil: BASE-B Experiment, *Journal of Geophysical Research*, **97** (D13), 14601- 14619, doi:10.1029/92JD01218.

Wooster, M. J., Gaveau, D, L, A., Salim, M. A., Zhang, T., Xu, W., Green, D. C., et al. (2018). New Tropical Peatland Gas and Particulate Emissions Factors Indicate 2015 Indonesian Fires Release Far More Particulate Matter (but Less Methane) than Current Inventories Imply. *Remote Sensing* **10**(4), 495. <https://doi.org/10.3390/rs10040495>.

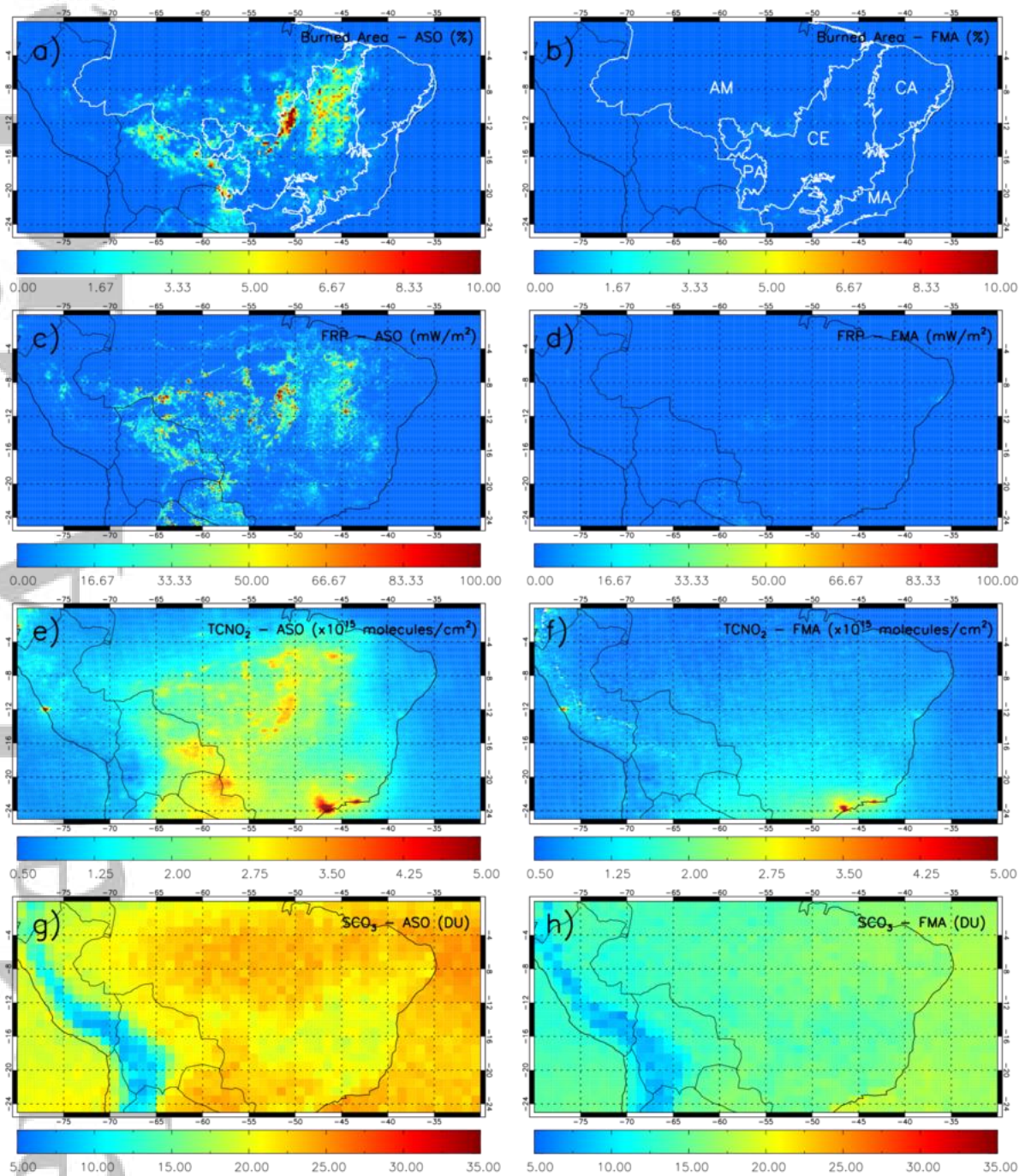


Figure 1: Mean satellite fire activity and tropospheric composition (2005-2016) for August-September-October (ASO; panels a, c, e and g) and February-March-April (FMA; panels b, d, f and h). Panels a) and b) show GFED Fire-Burned Area (FBA, %), panels c) and d) show GFAS Fire Radiative Power (FRP, mW/m²), panels e) and f) show OMI tropospheric column NO₂ (TCNO₂ - 10¹⁵ molecules/cm²) and panels g) and h) show OMI sub-column (0-6 km) ozone (Dobson units – DU). The

white-outlined regions in Figure 1a & b are the Brazilian biomes (Global Forest Watch, 2019) with their corresponding labels in red (AM=Amazonia, CA=Caatinga, CE=Cerrado, MA=Mata Atlantica and PA=Pantanal).

Accepted Article

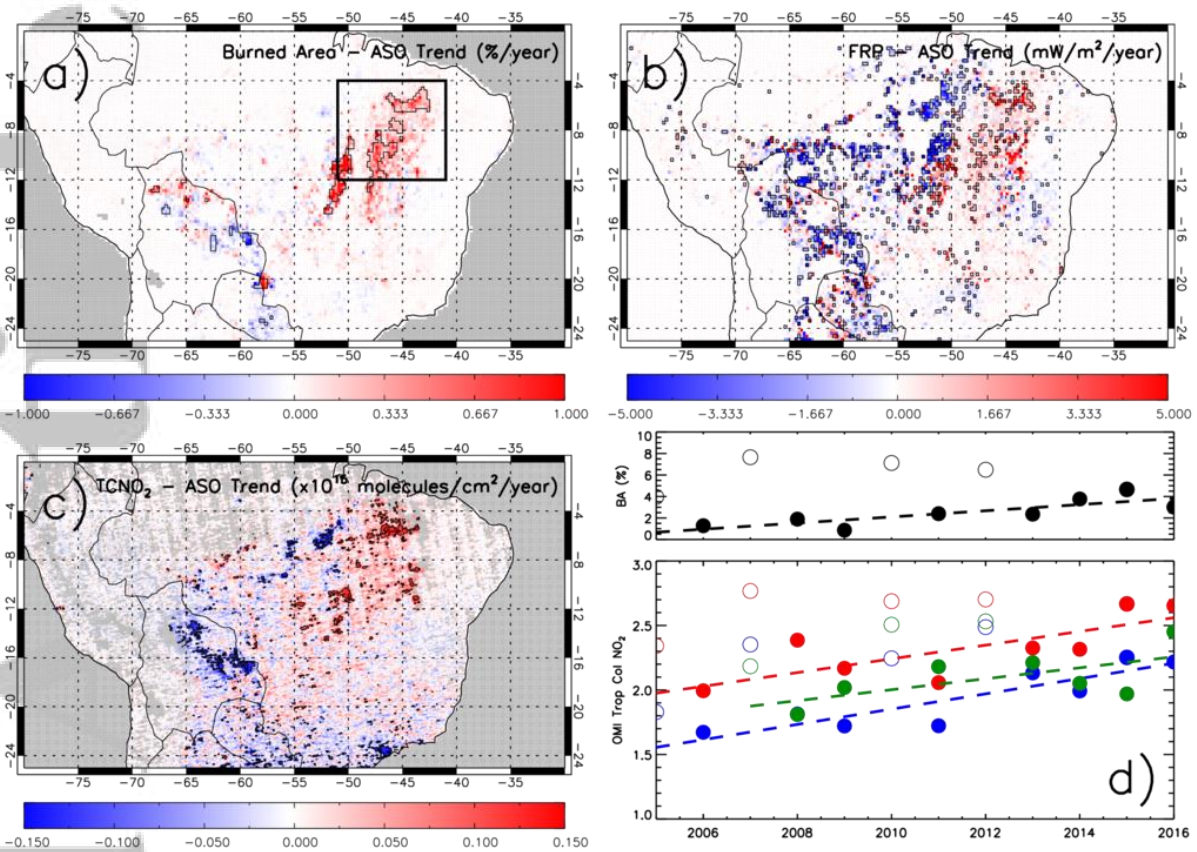


Figure 2: Linear trends in the burning-season (ASO) average for each year, between 2005 and 2016, for a) GFED FBA area fraction (%/year), b) GFAS FRP ($\text{mW}/\text{m}^2/\text{year}$) and c) OMI TCNO_2 (10^{15} molecules/ cm^2/year). Black polygon-outlined regions highlight significant trends at and above the 90% confidence level (>90%CL). Panel d) shows significant (>90% CL) regional trends (black box – 2a) in FBA (%/year), OMI TCNO_2 (10^{15} molecules/ cm^2/year), GOME-2 TCNO_2 (10^{15} molecules/ cm^2/year) and OMI TCNO_2 sampled under FBA area pixels of >1% (10^{15} molecules/ cm^2/year) represented by the black, blue, green and red dashed lines, respectively. Open circles represent extreme drought/anomalous fire (ED-AF) years, and are not included in trend analysis.

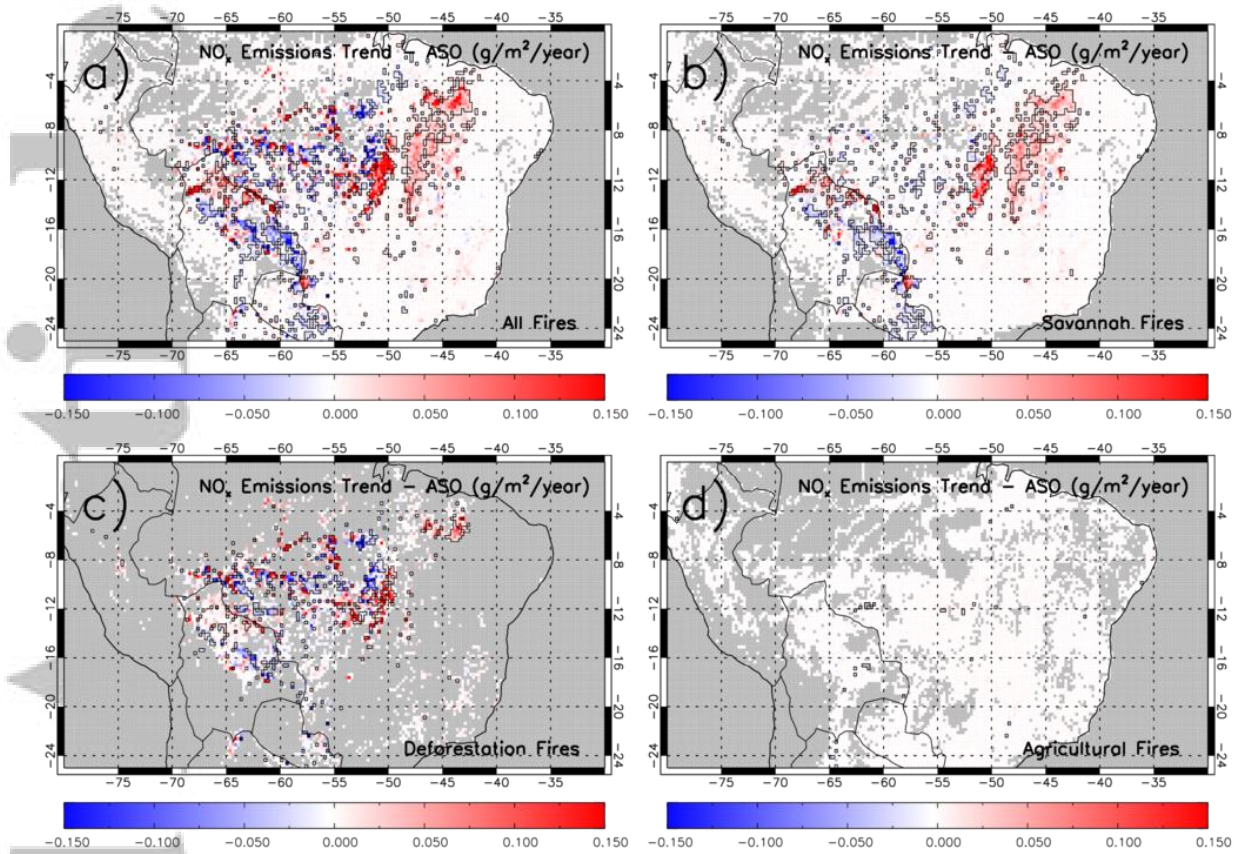


Figure 3: Trends in GFED NO_x (g/m²/year) ASO total emissions between 2005 and 2016 for a) all fires, b) savannah fires, c) deforestation fires and d) agricultural fires. Black polygon-outlined regions indicate significant trends above the 90% CL.

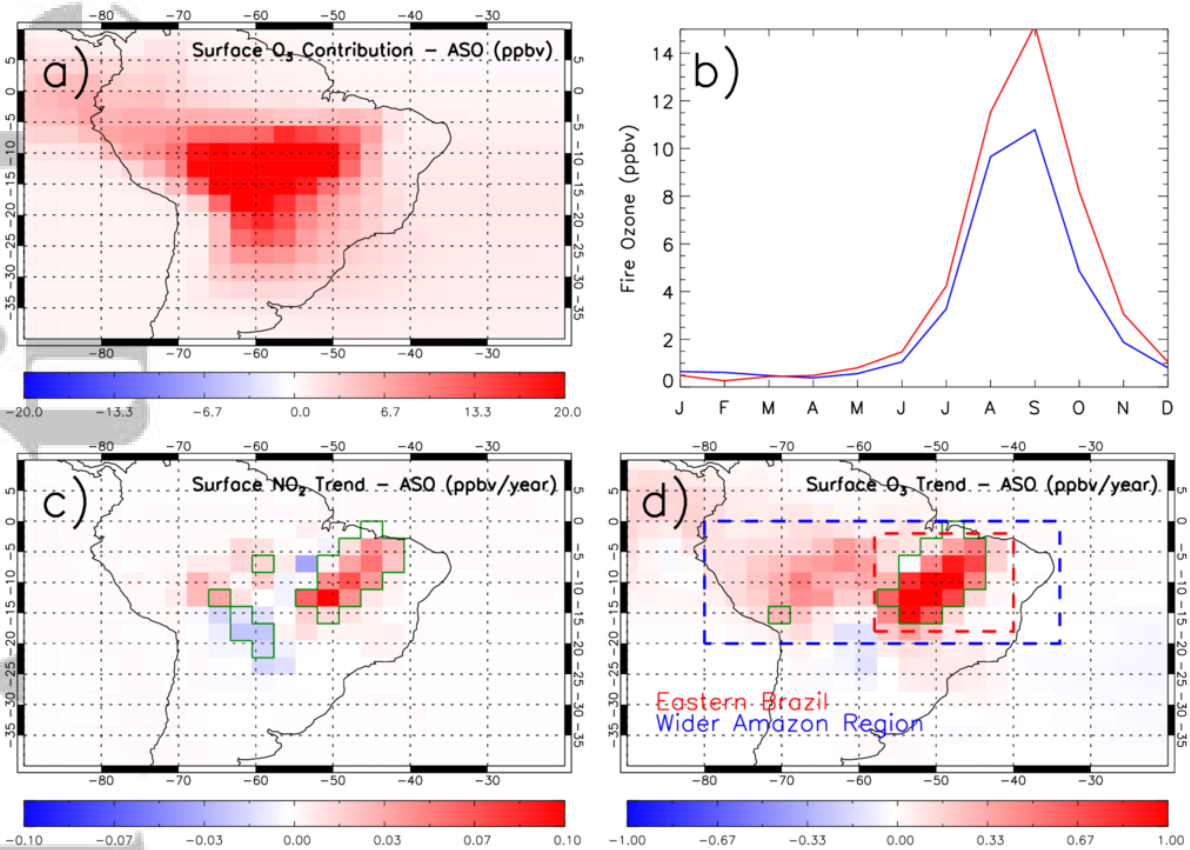


Figure 4: a) Average (ASO, 2005-2016) contribution of fire-sourced ozone to Amazon surface ozone concentrations (ppbv). b) Seasonal cycle in surface fire-sourced ozone (ppbv) in the Eastern Brazil and Wider Amazon regions (red and blue dashed regions in panel d). Trends in TOMCAT model surface c) NO₂ (ppbv/year) and d) ozone (ppbv/year) for the ASO average between 2005 and 2016. Green polygon-outlined areas show regions of significant trends above the 90% CL.